Active Sites on Mesoporous and Amorphous Silica Materials and Their Photocatalytic Activity: An Investigation by FTIR, ESR, VUV−UV and Photoluminescence Spectroscopies

Yoshitaka Inaki,[†] Hisao Yoshida,*[,†] Tomoko Yoshida,[‡] and Tadashi Hattori[†]

Department of Applied Chemistry, Graduate School of Engineering, Nagoya University, Nagoya 464-8603, Japan, and Center for Integrated Research in Science and Engineering, Nagoya University, Nagoya 464-8603, Japan

Received: March 15, 2002; In Final Form: June 18, 2002

Active sites for photometathesis on mesoporous silica materials, FSM-16 and MCM-41, and amorphous silica, which are generated by dehydroxylation of surface isolated hydroxyl groups at high temperature above 673 K, were investigated by some spectroscopies such as FTIR, ESR, VUV−UV, and photoluminescence. FTIR study revealed that the catalytic active sites are the sites exhibiting the IR bands at 891 and 910 cm^{-1}, which are known as a "strained siloxane bridge". The catalytic active sites generated on three kinds of silica materials have uniform activity, and higher activity over FSM-16 than MCM-41 and amorphous silica is attributed to the larger amount of active sites generated. ESR study suggested that the IR bands would be assigned to the radical sites, ≡Si−O· (NBOHC), which would be generated together with ·Si≡ (E′ center) by the dehydroxylation at high temperature, and the NBOHC photoexcited under UV light below ca. 390 nm would cause the photometathesis.

Introduction

Since the discovery of ordered mesoporous silica materials, MCM-41[1,2] and FSM-16[3,4] in the early of 1990s, much work has been devoted to the improvement of the synthesis condition, the development of the postsynthesis method, and the discovery of other mesoporous silica species such as HMS[5] and SBA-15.[6] These materials have regular nanometer-sized pores and high surface area, approximately 1000 $m^2\ g^{-1}$, and therefore have attracted a great deal of attention as new materials for catalysts. In most cases, attempts to generate catalytic activity have been made over mesoporous silica materials modified by heteroatoms[7,8] or functional groups.[9−12] On the other hand, very few reports describe the catalytic activity of unmodified mesoporous silica materials themselves. This is because silica materials are generally recognized to be catalytically inert. However, the activity of amorphous silica for some catalytic reactions[13−21] and photocatalytic reactions[22−28] has been reported. Recently, catalytic activity of unmodified mesoporous silica was also reported for some reactions, e.g., acidic catalyzation,[29−31] radical cracking,[32−34] and photooxidation of propene.[35] In these reports,[29−35] the activity of mesoporous silica was higher than that of amorphous silica.

Previously, we reported that unmodified FSM-16 has higher activity for photometathesis of propene[36−38] than does amorphous silica.[26,27] Photometathesis over silica materials is a very unique system, because transition metals such as Mo, Re, and W have been generally believed to be essential active elements required for metathesis,[39] except for the rare cases over nontransition metal catalysts.[40−44] As reported previously,[37] the photometathesis over silica can be devided into two photoreaction steps. In the first step, the active site on the silica surface is excited by UV light, and subsequently, propene is adsorbed on the photoexcited active site to form one of metathesis intermediates. The second step is the metathesis cycle to form the products through two types of intermediate under photoirradiation.

Since pretreatment at high evacuation temperature above 673 K is essential for the activation of silica materials,[27,28,36−38] the active sites have been tentatively proposed[37,38] to be the so-called "strained siloxane bridge" sites generated through dehydroxylation of isolated hydroxyl groups on the silica surface.[45−53] When the photometathesis activities were compared among three kinds of silica materials, FSM-16, MCM-41, and amorphous silica, their activities were in the following order: FSM-16 > MCM-41 > amorphous silica.[38] However, this order could not be explained simply by the extent of dehydroxylation,[38] and detailed investigations of the active sites were required. In the present study, we investigated the active sites for photometathesis on silica materials by using FTIR, ESR, VUV−UV−vis, and photoluminescence spectroscopies.

Experimental Section

Materials. Three kinds of silica samples were used in this study: mesoporous silica materials (FSM-16 and MCM-41) and amorphous silica, which were the same samples used in our previous study.[38] The FSM-16 sample was prepared from water glass (Wako) as a silica source and hexadecyltrimethylammonium bromide (Kishida) as a surfactant. The MCM-41 sample was prepared by using the same water glass and surfactant as for the FSM-16 sample. An Al-free MCM-41 sample was also prepared by using high purity water glass (Fuji silysia, Al 0.6 ppm, Fe 0.4 ppm). Synthesized precursors of mesoporous silica materials were calcined at 523 K in a flow of N_2 for 1 h and subsequently at 873 K in a flow of air for 5 h to remove the organic fraction.

X-ray diffraction patterns, N_2 adsorption isotherms and pore size distributions confirmed that the mesoporous silica materials

* Corresponding author: Phone: +81-52-789-4609. Fax: +81-52-789-3193. E-mail: yoshidah@apchem.nagoya-u.ac.jp.
[†] Department of Applied Chemistry.
[‡] Center for Integrated Research in Science and Engineering.

10.1021/jp025768f CCC: $22.00
Published on Web 08/10/2002

were correctly synthesized as reported.[1,3] Pore size distributions of all the mesoporous silica materials were narrow at ca. 3.1 nm. Surface areas of all the mesoporous silica materials were around 900 $m^2\ g^{-1}$. The purity of the FSM-16 and MCM-41 samples was examined by ICP emission spectrometry, and only a small amount of Al was present as a contaminant (Si/Al = 531 and 661, respectively) that would have originated from water glass as a silica source. In the Al-free MCM-41 sample, the Al content was negligible (Si/Al > 5000).

Amorphous silica was prepared by the sol−gel method from tetraethyl orthosilicate (TEOS), referring to the literature.[38,54] Surface area of the amorphous silica sample was 568 $m^2\ g^{-1}$, and the Al content was negligible (Si/Al > 5000).

Photometathesis Reaction Test. The photometathesis reaction test was carried out in the same way as the previous work.[38] Pretreatment of silica materials (200 mg) was performed in the reactor at various temperatures in 100 Torr O_2 for 1 h, followed by evacuation for 1 h at the same temperature. Reaction was carried out in a closed static system (100 μmol of propene in 115 cm^3) at ambient temperature under photoirradiation using a 250 W ultrahigh-pressure Hg lamp. Products were analyzed by gas chromatography. Since photometathesis of propene (eq 1) over silica occurred in high selectivity with a small amount of byproduct but-1-ene,[36] the conversion was defined as the sum of the yields of ethene and but-2-ene.

$$2C_3H_6 \xrightarrow[\text{r.t.}]{h\nu} C_2H_4 + 2C_4H_8 \qquad (1)$$

Spectroscopies. FTIR spectra were recorded on a JASCO FT/IR-300 spectrometer equipped with an in-situ cell. The in-situ cell has KBr window for IR beam, quartz window for UV irradiation, and the pretreatment part made by quartz. The cell was connected to a vacuum system. The sample powder was pressed by 30 kg cm^{-2} into a self-supported disk (5.0−10.0 mg cm^{-2}) and mounted on the sample holder. The sample disk was pretreated in the same way as done for the reaction test at the pretreatment part of the cell, then the sample was moved to the measuring part to record spectra at room temperature without exposure to air. Resolution was 2.0 cm^{-1}. In the case of the NH_3 adsorption experiment, the pretreated silica was exposed to NH_3 vapor (10 Torr) for 30 min at room temperature followed by evacuation for 30 min at room temperature. Photoirradiation to the sample in the IR cell was carried out through the quartz window using the 250 W ultrahigh-pressure Hg lamp. The wavelength of photoirradiation light was limited by using TOSHIBA UV-cut filters (UV-31, UV-37, and Y-43), which allow the transmission of the light with wavelength λ > 310, 370, and 430 nm, respectively (50% transmission at 310, 370, and 430 nm).

VUV−UV-vis absorption spectra (the region from vacuum UV to visible light) and photoluminescence spectra were recorded using the synchrotron radiation facility at the beam line 1B station (BL-1B) in UVSOR, Institute for Molecular Science, Okazaki, Japan, operated at electron energy of 750 MeV (100−230 mA). Synchrotron radiation was used through a 1 m Seya-Namioka monochromator. Photoluminescence spectra were measured by using a monochromator (Spex 270M or Jobin-Yvon HR320) and a photomultiplier (Hamamatsu R4220). After the powder sample was pretreated by the same manner as the reaction test, the sample was introduced into a quartz cell and sealed without exposure to air. Then, the quartz cell was attached to the sample holder in the stainless steel vacuum chamber, and the spectra were measured at room temperature.

TABLE 1: Results of Photometathesis over Silica Materials

run	samples [a]	Si/Al ratio	reaction time/h	conversion[b]/ %
1	FSM-16	531	1	9.73
2	MCM-41	661	1	4.32
3	amorphous silica	>5000	1	2.02
4	NH_3-treated FSM-16[c]	531	1	0.00
5[d]	MCM-41	661	8	15.9
6[d]	Al-free MCM-41	>5000	8	15.5

[a] Samples were pretreated at 1073 K before the reaction test. [b] Conversion is sum of the yields of ethene and butene. [c] The sample pretreated at 1073 K was exposed to NH_3 at room temperature for 30 min, and subsequently evacuated at room temperature for 30 min. After that, photometathesis of propene was carried out on that sample. [d] The light intensity of Hg lamp was lower than that of other runs, and therefore, conversion of run 5 was not eight times larger than run 2.

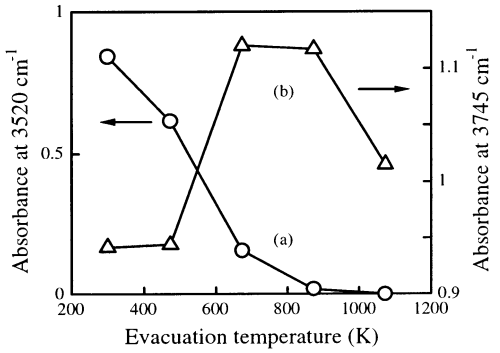

Figure 1. Absorbance of hydroxyl groups at 3520 (a) and 3745 cm^{-1} (b) on FTIR spectra of FSM-16 evacuated at various temperatures.

ESR spectra were recorded on a JEOL JES-TE200 (X-band). Measurement temperature is 77 K by using liquid nitrogen in a quartz Dewar. Microwave frequency was around 9.184 GHz, modulation width was 0.32 mT, time constant was 1 s, and microwave power was 1.0 mW. An in-situ cell having the pretreatment part and measurement part was employed. After the pretreatment of the sample, the sample was transferred to the measurement part made of quartz without exposure to air. The pretreatment of the sample was done in the same way as done for the reaction test. A ^1H NMR field meter was used for the determination of the magnetic field.

Results

Photometathesis Reaction Test. Table 1 shows the results of photometathesis of propene over silica materials activated by evacuation at 1073 K. As reported previously,[38] the activities on silica materials were in the following order: FSM-16 > MCM-41 > amorphous silica (runs 1−3). NH_3-treated FSM-16 exhibited no activity (run 4), suggesting that NH_3 deactivated the photometathesis active sites. In runs 5 and 6, both MCM-41 and Al-free MCM-41 exhibited almost the same conversion (15%), which is sufficiently less than the equilibrium conversion (35%),[27,36] suggesting that Al impurities do not influence the photometathesis activity.

Generation of the IR Bands due to "Strained Siloxane Bridge". With increasing the evacuation temperature, surface hydroxyl groups on silica materials are dehydroxylated, as is well known.[45] The IR spectrum of silica samples evacuated at room temperature exhibited a broad band with a top at 3520 cm^{-1} due to hydrogen bonded hydroxyl groups (adjacent hydroxyl groups; the left side of eq 2) and a sharp band at 3745 cm^{-1} due to isolated hydroxyl groups (the left side of eq 3). Figure 1 shows the variations of the IR band intensities of FSM-

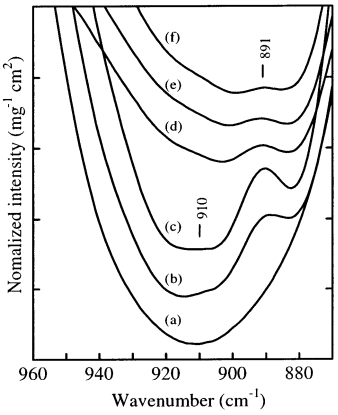

Figure 2. IR spectra of FSM-16 evacuated at (a) 673 K, (b) 873 K, and (c) 1073 K, and that of other silica materials evacuated at 1073 K (d) MCM-41, (e) Al-free MCM-41, and (f) amorphous silica.

16 with evacuation temperature. With increasing the evacuation temperature, the band of adjacent hydroxyl groups (3520 cm^{-1}) became gradually smaller (Figure 1a). With decreasing this band intensity, the band intensity due to isolated hydroxyl groups (3745 cm^{-1}) once increased at 673 K and then decreased, especially at 1073 K (Figure 1b). This means the reaction described as eq 2 proceeds predominantly below 673 K, then the reaction described as eq 3 occurs mainly at higher temperature. The longer distance between the isolated hydroxyl groups would require high temperature above 673 K for dehydroxylation.[38,45]

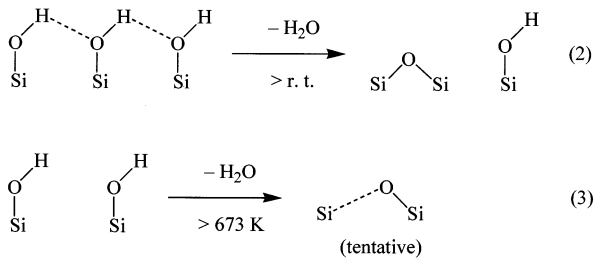

Accompanying the dehydroxylation of isolated hydroxyl groups above 673 K, new absorption bands appeared at 891 and 910 cm^{-1} in the transparent silica window (860−960 cm^{-1}), most clearly on the spectra of FSM-16 (Figure 2a−c). These two bands likely arose from dehydroxylation of isolated hydroxyl groups (Figure 1b), and so far they have been assigned to the so-called strained siloxane bridge (eq 3).[45−53] This site is suggested to be an unsymmetrical siloxane bond,[48] although the detailed structure has not been clarified.[55] Although the authors tentatively express this species as shown in the right side of eq 3, in accordance with the literature, the structure of this species will be discussed later. Except for these bands, no new bands appeared after evacuation at high temperature. The bands at 891 and 910 cm^{-1} were also observed on MCM-41 (Si/Al = 661), Al-free MCM-41, and amorphous silica after evacuation at 1073 K (Figure 2d−f). The band intensity was in the following order: FSM-16 > MCM-41 = Al-free MCM-41 > amorphous silica (Figure 2c−f).

Photoreaction between Propene and the Strained Siloxane Bridge. The effect of gaseous propene upon the site exhibiting the IR bands at 891 and 910 cm^{-1} was investigated on the FSM-16 sample, and the results are shown in Figure 3. The bands, which appeared after evacuation at 1073 K (Figure 3a), did not change in the dark for 60 min (not shown). Under photoirradiation (not shown) and after photoirradiation in the absence

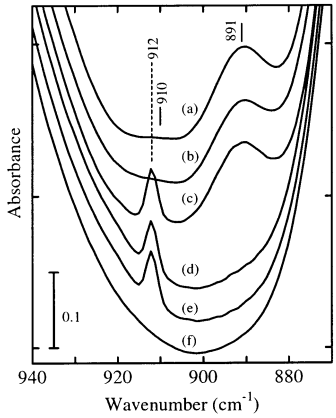

Figure 3. IR spectra of FSM-16 (a) evacuated at 1073 K and (b) that after subsequent photoirradiation for 120 min, (c) introduction of 15 Torr propene at r. t., (d) photoirradiation for 60 min in the presence of propene, (e) stored in the dark, and (f) evacuation of gaseous molecules. UV-cut filter was not used here.

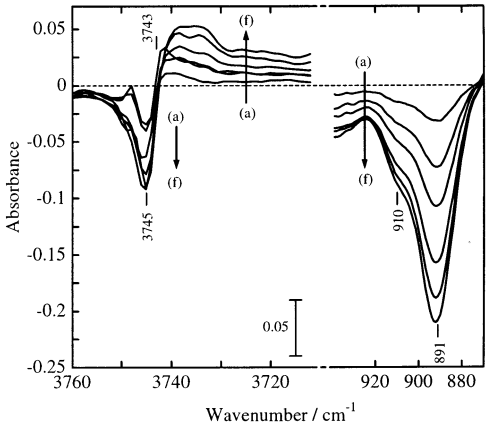

Figure 4. Variation of the difference IR spectra of FSM-16 evacuated at 1073 K with the photoirradiation time in the presence of propene. Irradiation time was (a) 10 min, (b) 30 min, (c) 50 min, (d) 90 min, (e) 130 min, and (f) 180 min. The each difference spectrum was obtained by subtracting the spectrum before irradiation from the spectra after photoirradiation.

of propene (Figure 3b), no changes were observed. Even when propene was introduced in the dark, nothing was changed (Figure 3c), except for the appearance of a sharp band at 912 cm^{-1} due to gaseous propene (out-of-plane CH_2 bending vibration mode[56]). On the other hand, the bands at 891 and 910 cm^{-1} disappeared when the sample was photoirradiated in the presence of propene (Figure 3d), when the photometathesis reaction should occur. After that, the spectrum did not vary in the dark for 60 min, (Figure 3e). After evacuation of gaseous molecules in the system, the band at 912 cm^{-1} due to gaseous propene disappeared completely, but the bands at 891 and 910 cm^{-1} were not recovered (Figure 3f). These results indicate that propene is chemisorbed on the sites under photoirradiation and that the photoirradiation is essential for this chemisorption.

Figure 4 shows variations of the IR spectrum of FSM-16 as difference spectra with photoirradiation time in the presence of propene. With increasing the photoirradiation time, the bands at 891 and 910 cm^{-1} became smaller. At the same time, the band at 3745 cm^{-1} due to isolated hydroxyl groups decreased and the broad band below 3743 cm^{-1} due to adjacent hydroxyl groups increased. These indicate that the density of surface hydroxyl groups increased and the sites decreased upon the photoirradiation in the presence of propene. These results might be because dissociative photoadsorption of propene occurred

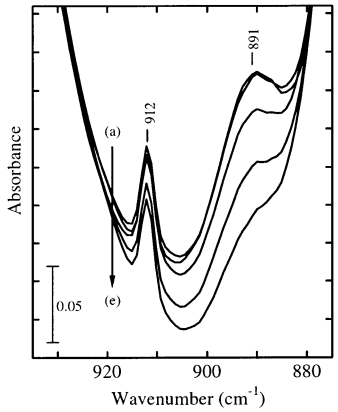

Figure 5. IR spectra of FSM-16 evacuated at 1073 K followed by (a) introduction of propene at r. t., (b) subsequent photoirradiation for 30 min through the filter Y-43, (c) UV-37, (d) UV-31, and (e) without the filter.

on the sites as shown in eq 4, although adsorbed C_3H_5 species were not detected.

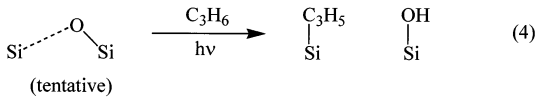

(4)

Figure 5 shows the effect of the wavelength of irradiation light on the photoadsorption of propene. When only visible light (λ > 430 nm) was irradiated on FSM-16 in the presence of propene, the bands at 891 and 910 cm^{-1} did not change (Figure 5b). On the other hand, irradiation of the light including the UV region (λ > 370 nm) caused a decrease in the intensity of the bands at 891 and 910 cm^{-1} (Figure 5c). When the wavelength region of the irradiation light was extended to the shorter UV region, the intensity decreased further (Figure 5d, 5e). These results indicate that the effective wavelength for the photoadsorption of propene on the sites is below ca. 370 nm in the UV region.

NH_3 Adsorption Study by FTIR Spectroscopy. NH_3 is a good probe for the strained siloxane bridge, since NH_3 is known to adsorb dissociatively on it, as shown in eq 5.[46−53] Exposing the evacuated silica materials to NH_3 caused complete disappearance of the bands at 891 and 910 cm^{-1} (not shown). At the same time, the band due to hydroxyl groups below 3743 cm^{-1} became larger (not shown) and some new bands appeared such as an intense band at 1553 cm^{-1} and small bands at 1623 and 1455 cm^{-1} (Figure 6), in addition to other intense bands at 3525 and 3444 cm^{-1} and small bands at 3400 and 3310 cm^{-1} (not shown). Three intense bands at 3525, 3444, and 1553 cm^{-1} were assigned to asymmetric stretching, symmetric stretching, and bending vibration modes of NH_2 in $SiNH_2$, respectively.[46−49,57,58] Generation of $SiNH_2$ and SiOH bands has been explained by the reaction of eq 5, as reported by Morrow et al.[46−49] The $SiNH_2$ bands became larger with a rise of the preevacuation temperature for FSM-16 prior to the adsorption of NH_3 (Figures 6a−c), and the same phenomena were also observed on MCM-41, Al-free MCM-41, and amorphous silica. The intensities of the $SiNH_2$ bands among silica materials were in the following order: FSM-16 > MCM-41 = Al-free MCM-41 > amorphous silica (Figures 6a, d−f).

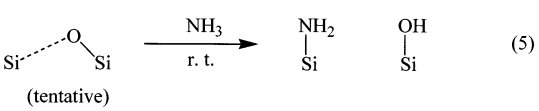

(5)

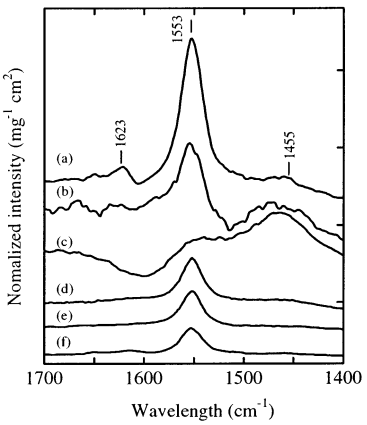

Figure 6. Difference IR spectra after exposure to NH_3 at r. t. for FSM-16 evacuated at (a) 1073 K, (b) 873 K, and (c) 673 K, and for other silica materials, (d) MCM-41, (e) Al-free MCM-41, and (f) amorphous silica evacuated at 1073 K. These were obtained by subtracting the spectrum before NH_3 adsorption from the spectrum after NH_3 adsorption.

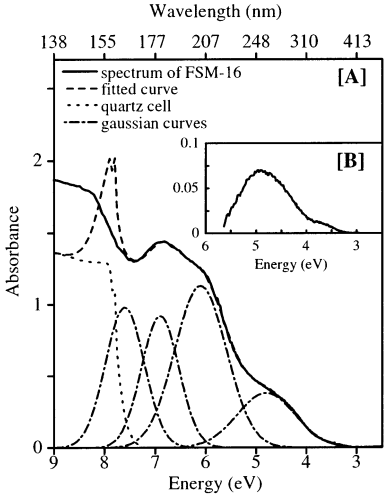

Figure 7. (A) VUV−UV-visible spectrum of FSM-16 evacuated at 1073 K for 1 h. The spectrum was fitted by a curve of the quartz cell and four Gaussian curves at 7.6, 6.9, 6.0, and 4.8 eV. Curve fitting above 7.6 eV did not work, because a large band of the band gap of silica existed and transmittance was low. (B) The difference spectrum obtained by subtracting the spectrum of FSM-16 evacuated at 1073 K in the presence of propene from that after photoirradiation (the same spectrum was in ref 37).

The band at 1455 cm^{-1} could be assigned to NH_4^+ species on the Brønsted acid sites.[59] The bands at 3400, 3310, and 1623 cm^{-1} could be assigned to the NH_3 on the hydroxyl groups.[60] As for the band at 1623 cm^{-1}, a band originated from coordinated NH_3 to Lewis acid sites would be overlapped.[59,60] Brønsted acid and Lewis acid sites would be originated from the small content of Al in FSM-16 (Si/Al = 531) and MCM-41 (Si/Al = 661).

Photoabsorption and Photoluminescence Sites on Evacuated Silica. Figure 7A shows the VUV−UV-vis absorption spectrum of the FSM-16 sample evacuated at 1073 K. The spectrum shows complex bands less than ca. 390 nm (> 3.2 eV). Similar spectra were obtained on MCM-41 and amorphous silica. The absorption region of the quartz cell was in agreement with the band gap of bulk silica at 153 nm (8.1 eV).[23] Complex bands in an energy region lower than the band gap could be fitted[61] by four Gaussian curves centered at 163 nm (7.6 eV), 180 nm (6.9 eV), 203 nm (6.1 eV), and 258 nm (4.8 eV); these

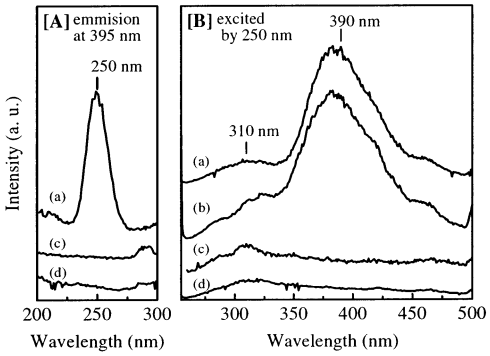

Figure 8. Photoexcitation (A) and photoemission (B) spectra of (a) FSM-16, (c) MCM-41, and (d) amorphous silica evacuated at 1073 K. The photoexcitaion spectra (A) were measured by monitoring the emission light at 395 nm, and the photoemission spectra (B) were measured by the excitation light at 250 nm. The emission spectrum (Bb) was of the FSM-16 sample after photoirradiation for 15 min in the presence of propene.

energy positions were determined by using examples from literature.[62] These bands of silica were assigned to several optically active oxygen-deficiency-related centers, and they are well reviewed by Skuja.[62] The former three bands represent the Si−Si bond species (≡Si−Si≡) or oxygen vacancy for the band at 163 nm, oxygen vacancy at 180 nm, and surface E′ center (≡Si•) for 203 nm, respectively, where "≡" denotes three bonds with oxygen, and " • " represents the unpaired spin. However, some candidates could be listed for the last one at 258 nm, e.g., ≡Si−O• (nonbridging oxygen hole center (NBOHC)), ═Si: (two-coordinated silicon ($B_2\beta$ center)), ≡Si−O−O• (peroxy radical (POR)),[62] where "═" denote two bonds with oxygen. This lowest energy band (258 nm) shows the absorption edge at ca. 390 nm (3.2 eV). In our previous study,[37] it was confirmed that the intensity of the absorption band generated on FSM-16 was reduced by the adsorption of propene under the light below ca. 370 nm. The difference spectrum[37] obtained by subtracting the spectrum after the photoadsorption of propene from that before photoadsorption was depicted in Figure 7B. The effective wavelength for photometathesis was evaluated to be λ < 390 nm from the difference spectrum. The difference spectrum is quite similar to the lowest band at 4.8 eV in Figure 7A.

Figure 8 shows the photoluminescence spectra of silica materials evacuated at 1073 K. FSM-16 exhibited two emission peaks at 310 and 390 nm (Figure 8Ba), when the excitation light was at 250 nm (Figure 8Aa). These emission bands could be assigned to ═Si: ($B_2\beta$).[62−64] The emission from the $B_2\beta$ center on FSM-16 was also observed after photoirradiation in the presence of propene (Figure 8Bb), in which photometathesis should proceed. This indicates that propene cannot react with the $B_2\beta$ center under photoirradiation. Moreover, exposure to NH_3 did not affect the $B_2\beta$ emission band (not shown), indicating no relationship between the $B_2\beta$ center and the active sites. As for MCM-41 and amorphous silica, no emission peaks at 390 nm were observed (Figure 8Bc, 8Bd).

Generation of the Radical Sites on Evacuated Silica. Figure 9 shows the ESR spectra of silica materials evacuated at high temperatures, which were recorded at 77 K. Although Morrow et al. reported that radical species were not observed on amorphous silica evacuated at high temperature,[53] in the present study some kinds of radical species were observed on silica materials, most clearly on FSM-16. The signals became larger when the evacuation temperature was increased. Four kinds of

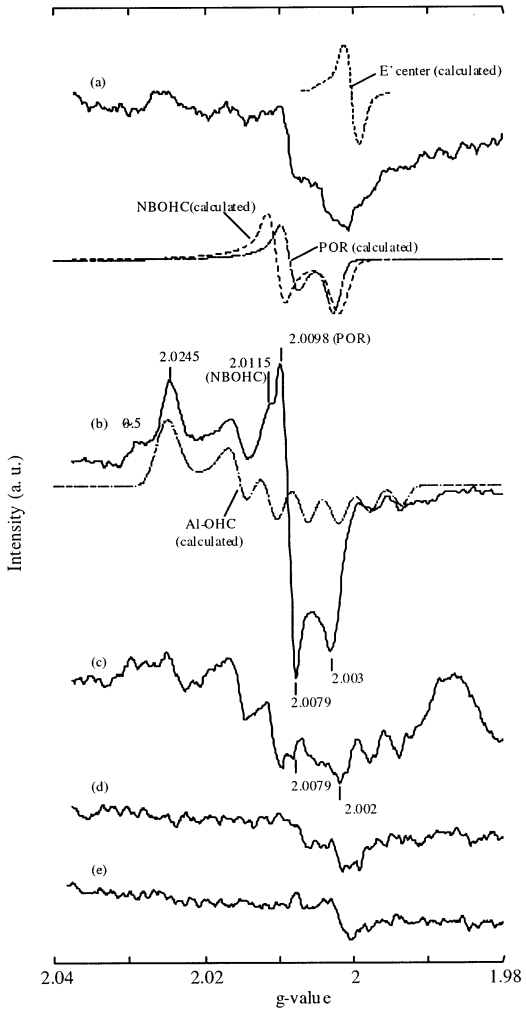

Figure 9. ESR spectra of FSM-16 evacuated at (a) 873 K and (b) 1073 K, and (c) the spectrum of MCM-41 evacuated at 1073 K, of amorphous silica evacuated at (d) 1073 K, and (e) of the quartz cell. The spectra of NBOHC, POR, Al−OHC, and E′ center were also depicted.

calculated signals due to defect centers were also shown in Figure 9: ≡Si−O• (NBOHC (nonbridging oxygen hole center), $g_1 = 2.0010$, $g_2 = 2.0095$, g_3 (less intense) = 2.078),[62,63,65] ≡Si−O−O• (POR (peroxy radical), $g_1 = 2.0018$, $g_2 = 2.0078$, g_3 (less intense) = 2.067),[62,63,65] ≡Al−O• (Al−OHC (Al oxygen hole center), $g_1 = 2.0043$, $g_2 = 2.0080$, $g_3 = 2.024$, $A_{xx} = 7.0$ G, $A_{yy} = 3.0$ G, $A_{zz} = 0.5$ G),[66,67] and ≡Si(E′ center, $g_\perp = 2.001$, $g_{//} = 2.002$).[62,63] These signals could be observed even at room temperature, although the intensities of the spectra were very small. The spectrum of FSM-16 (Figure 9a and 9b) seemed to consist of four kinds of signals: NBOHC, POR, Al−OHC, and E′ center. The shape of Al−OHC signal having hyperfine structure due to $I = 5/2$ of ^{27}Al is similar to that of $CaO-Al_2O_3-SiO_2$,[66] and that of quartz,[68] although the g value is slightly different. With increasing the evacuation temperature (from the curve 9a to 9b), these signals on FSM-16 became larger, although E′ center became unclear due to the overlap of other large three signals.

The spectrum of MCM-41 would also consist of four signals (Figure 9c), but the Al−OHC signal was dominantly observed. The spectrum of amorphous silica might consist of three kinds of signals other than Al−OHC, but these were very small (Figure 9d). Although the precise comparison of the band intensities among these spectra could not be allowed, the order

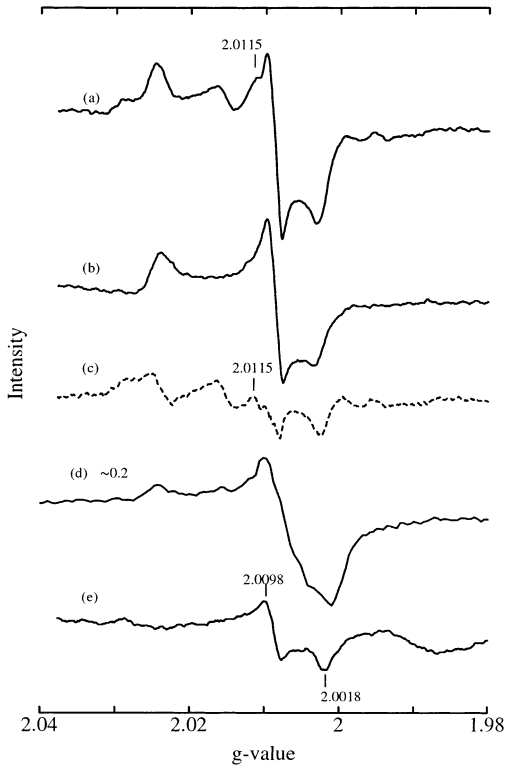

Figure 10. Series of ESR spectra of FSM-16. The spectrum (a) was of the sample evacuated at 1073 K. The spectrum (b) was after photoirradiation at 77 K through the glass filter UV-37. The difference spectrum (c) was obtained by subtracting the spectrum (b) from (a). The spectrum (d) was after exposure to O_2 on (a) for 10 min at r. t. followed by evacuation at r. t. for 10 min. The spectrum (e) was after exposure to NH_3 at r. t. on (a) for 30 min followed by evacuation at r. t. for 30 min. All spectra were measured at 77 K.

of signal intensity was roughly estimated to be as follows: FSM-16 > MCM-41 > amorphous silica (Figures 9b, c and d).

Under photoirradiation, the signals of NBOHC, POR, and Al−OHC became smaller (Figure 10b, see also difference spectrum in Figure 10c). Almost the same results were observed under the light from the UV region to ca. 660 nm, and shorter UV light was more effective. This result is because these sites were photoexcitated by UV and visible light and a part of the sites lost the radical property under the light. To confirm the reactivity of radical sites, O_2 or NH_3 gas was introduced. When O_2 gas was introduced on FSM-16 evacuated at 1073 K, very large signal due to POR appeared (Figure 10d). After the introduction of NH_3 gas at room temperature on the evacuated FSM-16, the signals of NBOHC, Al−OHC, and E′ center almost disappeared (Figure 10e), and only the signal of POR remained. These responses to O_2 or NH_3 were similarly observed on all silica materials evacuated above 673 K.

Discussion

Identification of Photometathesis Active Sites. In our previous study,[37,38] it was proposed that the photoabsorption sites detectable in UV-vis spectra (λ_{max} at 250 nm, edge at 390 nm) are the active sites for photometathesis, since good agreements between the results from UV-vis spectroscopy and the reaction test were observed in the following three features. (i) With increasing the evacuation temperature above 673 K, the photoabsorption sites appeared and the reaction activity increased. (ii) Upon photoirradiation, propene was adsorbed by the photoabsorption sites as shown in Figure 7B, and the reaction proceeded. (iii) The effective wavelength of irradiation light was below ca. 370 nm for both the photoadsorption of propene on the photoabsorption sites and the progress of the reaction, and that was in good agreement with the wavelength region of the photoadsorptin band as shown in Figure 7B.

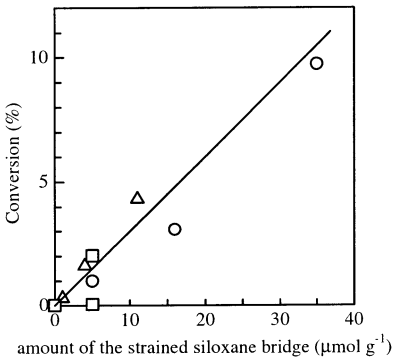

Figure 11. Plot of the photometathesis conversion of propene against the amount of the sites on FSM-16 (○), MCM-41 (△), and amorphous silica (□) evacuated at various temperatures.

The present IR study suggested that the sites exhibiting the IR bands at 891 and 910 cm^{-1} would be the photometathesis active sites, since the three features listed above agree well with the following present results in IR spectroscpy. (i) With increasing the evacuation temperature above 673 K, the intensity of the IR bands at 891 and 910 cm^{-1} increased (Figure 2, eq 3). (ii) The IR bands disappeared when the adsorption of propene occurred under photoirradiation (Figures 3−5). (iii) The effective wavelength for the disappearance of the bands was below ca. 370 nm (Figure 5). In addition to these agreements, NH_3 treatment deactivated the photometathesis activity (Table 1), while the NH_3 molecule adsorbed dissociatively on the sites (Figure 6, eq 5).

From above, it could be concluded that the sites exhibiting the IR bands at 891 and 910 am^{-1} are the active sites for the photometathesis. Probably, photoabsorption of UV light below ca. 370 nm by the sites causes the dissociative adsorption of propene on the sites (eq 4) and subsequent formation of metathesis intermediates. It is noteworthy that the acid sites (Figure 6) are not the photometathesis active sites, since MCM-41 (Si/Al = 661) and Al-free MCM-41 (Si/Al > 5000) exhibited almost the same activity (Table 1) and the same intensity of the IR bands (Figure 2).

Quantitative Interpretation of Photometathesis Activity. Photometathesis activities over three kinds of silica materials were in the following order: FSM-16 > MCM-41 > amorphous silica (Table 1, also as reported in ref 38). Since this order is in good agreement with that of the intensities of the IR bands at 891 and 910 cm^{-1} on the silica materials (Figure 2), the photometathesis activity is expected to depend on the amount of the bands regardless of the structure of the silica materials.

It was difficult to estimate the amount of the sites precisely from the integrated intensity of the IR bands at 891 and 910 cm^{-1} (Figure 2), because the baseline in the silica window (860−960 cm^{-1}) is not static. Since the sites are very sensitive for the adsorption of NH_3 (eq 5), the amount of the sites could be estimated from the integrated intensity of $SiNH_2$ band at 1553 cm^{-1} (Figure 6) by using the absorption coefficient[12] of the band.

Figure 11 shows the relationship between the amount of the sites and the photometathesis conversion over three kinds of silica materials evacuated at various temperatures. The activity seemed to be proportional to the amount of the sites. This result

demonstrates quantitatively that the sites exhibiting the bands at 891 and 910 cm^{-1} are the active sites for photometathesis. In addition, this indicates that all the generated active sites have essentially uniform activity for photometathesis, regardless of the kinds of silica materials and the evacuation temperatures. This means that the activity depends not on the specific activity of the sites but on the amount of the sites; the higher activity of FSM-16 than of the other silica materials is attributed to the larger amount of the active sites.

We estimated a turnover number (TON), which was defined as TON = (the number of the converted propene to ethene and butenes)/(the number of the active sites), where as the number of the catalytic active sites we employed the number of the sites estimated by the band intensity at 1553 cm^{-1} after NH_3 adsorption. In the present system, the propene photometathesis reaches equilibrium at the propene conversion of ca. 35%.[27,36] The reaction over FSM-16 evacuated at 1073 K (Table 1) also reached equilibrium after being irradiated for a long time, meaning that at least 35 μmol of propene converted to ethene and butene (eq 1). Since this sample contained 35 μmol g^{-1} of the active sites (Figure 11) and the sample used in the reactor was 0.2 g, the number of the active sites was calculated to be 7 μmol. Thus, TON was calculated to be 5.0 at least in this case. Under different reaction conditions, the highest TON confirmed so far was calculated to be 28. These indicate that the photometathesis reaction over silica materials proceeds *catalytically*.

Structure and Photoreactivity of the Active Sites. As mentioned above, the photometathesis active sites were concluded to be the sites exhibiting the IR bands at 891 and 910 cm^{-1}. Morrow et al. assigned the IR bands at 888 and 908 cm^{-1} to the strained siloxane bridge. They reported that the strained siloxane bridge is an asymmetric siloxane bond where one of the silicon atoms may be electron deficient,[46] but it is not a radical site because no ESR signals were observed.[53] Bunker et al. proposed the edge-shared silicate tetrahedra (eq 6) as a model of the strained siloxane bridge.[50,51] The edge-shared silicate tetrahedra would have a high activity, but, their IR vibration modes estimated by MO calculation did not agree with that of the strained siloxane bridge.[50] Although much investigation has been done for the strained siloxane bridge, its structure has not been clarified yet, as pointed out by Morrow.[55]

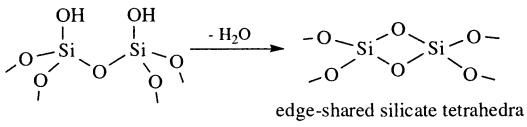

(6)

In the present ESR study, some radical species, such as NBOHC (≡Si−O·), E′ center (≡Si·), Al−OHC (≡Al−O·), and POR (≡Si−O−O·), were generated on the silica materials by evacuation at high temperature above 673 K (Figure 9), contrary to the report by Morrow.[53] Among these paramagnetic sites, NBOHC shows some features in common with the photometathesis active site exhibiting the IR bands at 891 and 910 cm^{-1}. (i) Evacuation at high temperature was required for the generation of both sites (Figures 2 and 9). (ii) The amount of both sites is greater on FSM-16 than on MCM-41 and amorphous silica (Figures 2 and 9). (iii) NBOHC is known to show the absorption band at 4.8 eV (258 nm) and 2.0 eV (620 nm),[57,59] and the former wavelength is in agreement with the effective wavelength region in photometathesis (Figures 5 and 7B, and ref 37). Such photoexcitation of NBOHC was confirmed by the decrease in the intensity under UV and visible light (Figures 10b and c). In the photoexcited state, NBOHC would not have the radical feature (eq 7), since it was suggested that the generated hole on Si is transferred to surrounding oxygen.[66−71] (iv) Introduction of NH_3 leads to the disappearance of both the IR bands (Figure 6) and the NBOHC signal (Figure 10e). (v) Skuja reported that the symmetric vibration mode of ≡Si−O· is 890 cm^{-1} observed by laser induced photoemission spectrum,[69−71] and this value is almost the same as the vibration frequency of the strained siloxane bridge (888−910 cm^{-1}). These common features suggest that NBOHC is the site exhibiting the IR bands at 891 and 910 cm^{-1}, which have been assigned to the strained siloxane bridge so far, and at the same time NBOHC would be the photometathesis active site.

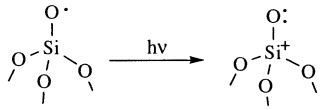

(7)

It has been frequently reported that the strained Si−O bond could be cleaved homolytically. For example, the strained Si−O−Si bond is cleaved to form ≡Si−O· + ·Si≡ under laser, γ-ray, or neutron irradiation,[72,73] and the same cleavage occurred during the rapid quenching in the drawing process of the glass fiber.[63,74] Moreover, Glinka et al.[75] proposed an idea that dehydroxylation of SiOH groups on MCM-41 above 873 K could produce radical pair sites by a reaction such as described by eq 8 without ESR spectrum. In the present study, the E′ center was also generated by evacuation at high temperature above 673 K together with NBOHC (Figures 7 and 9). Thus, dehydroxylation of isolated hydroxyl groups is suggested to induce the formation of two radical sites, ≡Si−O· and ·Si≡ (eq 8).

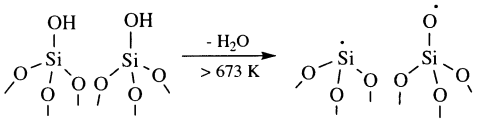

(8)

Other Candidates for the Active Sites. The effective wavelength region for photometathesis is around at 250 nm (Figure 7B).[37] The generated species other than NBOHC also could exhibit absorption in such wavelength region; POR shows absorption bands at 4.8 eV (258 nm) and 2.0 eV (620 nm),[62,63] the $B_2\beta$ center also shows an absorption band at 4.8 eV (258 nm),[62−64] and the absorption band of Al−OHC is proposed to be at 3.9 eV (318 nm).[67] These absorption bands would overlap with the band of NBOHC at 4.8 eV in Figure 7A. However, these can be excluded from the list of candidates for the active sites for the following reasons. A large signal due to POR was formed after introduction of O_2 on the evacuated silica (Figure 10d), but O_2 deactivates the photometathesis reaction as described in our previous study.[35] The $B_2\beta$ center was observed only on FSM-16 and not on MCM-41 and amorphous silica (Figures 8a, c, and d), and the $B_2\beta$ center is active neither on the propene molecule under photoirradiation (Figure 8b), nor on the NH_3 molecule. The absorption band due to Al−OHC observed in ESR (Figure 9) is at 3.9 eV (318 nm)[66,67] and close to the band due to active sites. However, Al−OHC would have no activity for photometathesis because the activities were almost the same between Al-free and Al−MCM-41 (Table 1).

In addition, Matsumura et al. reported that the paramagnetic site, ≡Si−O−−Si≡, which can be photoexcited by UV light,

SCHEME 1

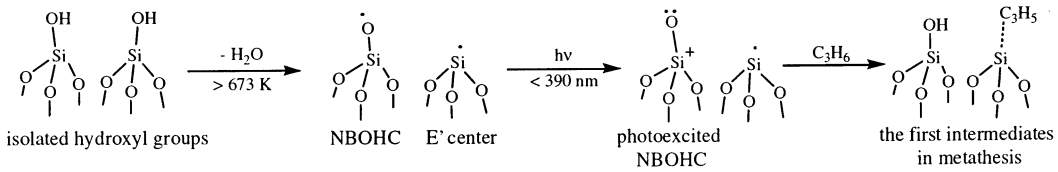

was formed by evacuation above 950 K.[19] However, the signals in our ESR study were different from that of such site.

Reaction Scheme of Propene Photometathesis. As mentioned above, the photometathesis active sites generated by evacuation at high temperature are the sites showing IR bands at 890 and 910 cm^{-1}. The sites would correspond to the radical sites ≡Si−O· (NBOHC) that would be generated together with ·Si≡ (E′ center). Scheme 1 summarizes the generation step of the active sites and initial photoexcitation step of photometathesis. NBOHC is formed through dehydroxylation and photoexcited by absorption of UV light below around 390 nm (Figures 7A and 7B). Then, propene is adsorbed on the photoexcited NBOHC, followed by further conversion into a metathesis intermediate that would be one of two types of intermediates formed.[37] The details about the intermediates in this system have not been clarified yet.

As described above, ≡Si−O· can be photoexcited under the light at 4.8 eV (258 nm) and 2.0 eV (620 nm).[62,63,69−71] The former (4.8 eV, 258 nm) corresponds to a charge transfer from bonding orbital of Si−O to 2p nonbonding orbital of nonbridging oxygen (≡Si−O· → (≡Si^{+}−O:)*). The latter (2.0 eV, 620 nm) corresponds to a charge transfer from a 2p nonbonding orbital of oxygen connecting to Si−O· to a 2p nonbonding orbital of nonbridging oxygen (O_3Si−O· → (O_3^{+}Si−O:)*). In the present case, only the former excitation would induce the metathesis reaction. The latter excitation would not be enough to activate the propene molecules into photometathesis intermediates, because the reaction proceeds only under UV light.

Conclusion

The catalytic active sites for photometathesis on mesoporous silica, FSM-16 and MCM-41, and amorphous silica were revealed. The active sites are generated by dehydroxylation of isolated hydroxyl groups at high temperature, and they exhibit IR bands at 891 and 910 cm^{-1}, which have been assigned to so-called "strained siloxane bridge". In this study, the IR bands were suggested to be assigned to the radical site, NBOHC (≡Si−O·) that is generated together with the E′ center (·Si≡). NBOHC is photoexcited under light below ca. 390 nm and reacts with propene to promote the photometathesis catalytically.

The active sites on silica materials, FSM-16, MCM-41, and amorphous silica, have a uniform activity for photometathesis. The higher activity of FSM-16 than MCM-41 and amorphous silica is attributed to the larger amount of the active sites generated on FSM-16.

Acknowledgment. The authors thank Assistant Professor Atsushi Satsuma for the valuable discussion, and thank Mr. Toshiei Watanabe and Tatsumi Imura for making the in-situ IR cell. VUV−UV-vis absorption and photoluminescence measurements were done as the part of the Joint Studies Program (1999, 2000) of UVSOR of the Institute for Molecular Science. This work was partly supported by Nippon Sheet Glass Foundation for Materials Science and Engineering.

References and Notes

(1) Beck, J. S.; Vartuli, J. C.; Roth, W. J.; Leonowicz, M. E.; Kresge, C. T.; Schmitt, K. D.; Chu, C. T−W.; Olson, D. H.; Sheppard, E. W.; McCullen, S. B.; Higgins, J. B.; Schlenker, J. L. *J. Am. Chem. Soc.* **1992**, *114*, 10834.

(2) Kresge, C. T.; Leonowicz, M. E.; Roth, W. J.; Vartuli, J. C.; Beck, J. S. *Nature* **1992**, *359*, 710.

(3) Inagaki, S.; Fukushima, Y.; Kuroda, K. *J. Chem. Soc., Chem. Commun.* **1993**, 680.

(4) Inagaki, S.; Koiwai, A.; Suzuki, N.; Fukushima, Y.; Kuroda, K. *Bull. Chem. Soc. Jpn.* **1996**, *69*, 1449.

(5) Tanev, P. V.; Chibwe, M.; Pinnavia, T. J. *Nature* **1994**, *368*, 321.

(6) Yang, P.; Zhao, D.; Margolese, D. I.; Chmeika, B. F.; Stucky, G. D. *Nature* **1998**, *396*, 152.

(7) Corma, A. *Chem. Rev.* **1997**, *97*, 2373.

(8) Ying, J. Y.; Mehnert, C. P.; Wong, M. S. *Angew. Chem., Int. Ed. Engl.* **1999**, *38*, 56.

(9) Brunel, D. *Microporous Mesoporous Mater.* **1999**, *27*, 329.

(10) Anwander, R.; Nagl, I.; Widenmeyer, M.; Engekhardt, G.; Groeger, O.; Palm, C.; Röser, T. *J. Phys. Chem. B* **2000**, *104*, 3532.

(11) Dapaah, J. K. A.; Uemichi, Y.; Ayame, A.; Matsuhashi, H.; Sugioka, M. *Chem. Lett.* **2000**, 604.

(12) Inaki, Y.; Kajita, Y.; Yoshida, H.; Ito, K.; Hattori, T. *Chem. Commun.* **2001**, 2358.

(13) Armor, J. N.; Zambri, P. M. *J. Catal.* **1982**, *73*, 57.

(14) Lacroix, M.; Pajonk, G. M.; Teichner, S. J. *J. Catal.* **1986**, *101*, 314.

(15) Kastanas, G. N.; Tsigdinos, G. A.; Schwank, J. *J. Appl. Catal.* **1988**, *44*, 33.

(16) Kasztelan, S.; Moffat, J. B. *J. Catal.* **1987**, *106*, 512.

(17) Vikulov, K.; Martra, G.; Coluccia, S.; Miceli, D.; Arena, F.; Parmaliana, A.; Paukshtis, E. *Catal. Lett.* **1996**, *37*, 235.

(18) Matsumura, Y.; Hashimoto, K.; Yoshida, S. *J. Catal.* **1989**, *117*, 135.

(19) Matsumura, Y.; Moffat, J. B.; Hashimoto, K. *J. Chem. Soc., Faraday Trans.* **1994**, *90*, 1177.

(20) Bittner, E. W.; Bockrath, B. C.; Solar, J. M. *J. Catal.* **1994**, *149*, 206.

(21) Morikawa, A.; Hattori, M.; Yagi, K.; Otsuka, K. *Z. Phys. Chem., N. F.* **1977**, *140*, 309.

(22) Anpo, M.; Yun, C.; Kubokawa, K. *J. Catal.* **1980**, *61*, 267.

(23) Kubokawa, Y.; Anpo, M.; Yun, C. *Proc. 7th Int. Congress Catal.* (*B*) **1980**, 1171.

(24) Ogata, A.; Kazukawa, A.; Enyo, M. *J. Phys. Chem.* **1986**, *90*, 5201.

(25) Yoshida, H.; Tanaka, T.; Yamamoto, M.; Funabiki, T.; Yoshida, S. *Chem. Commun.* **1996**, 2125.

(26) Yoshida, H.; Tanaka, T.; Yamamoto, M.; Yoshida, T.; Funabiki, T.; Yoshida S. *J. Catal.* **1997**, *171*, 351.

(27) Yoshida, H.; Tanaka, T.; Matsuo, S.; Funabiki, T.; Yoshida, S. *J. Chem. Soc., Chem. Commun.* **1995**, 761.

(28) Tanaka, T.; Matsuo, S.; Maeda, T.; Yoshida, H.; Funabiki, T.; Yoshida, S. *Appl. Surf. Sci.* **1997**, *121/122*, 296.

(29) Yamamoto, T.; Tanaka, T.; Funabiki, T.; Yoshida, S. *J. Phys. Chem. B* **1998**, *102*, 5830.

(30) Tanaka, Y.; Sawamura, N.; Iwamoto, M. *Tetrahedron Lett.* **1998**, *39*, 9457.

(31) Yamamoto, T.; Tanaka, T.; Inagaki, S.; Funabiki, T.; Yoshida, S. *J. Phys. Chem. B* **1999**, *103*, 6450.

(32) Hattori, T.; Ebigase, T.; Inaki, Y.; Yoshida, H.; Satsuma, A. *Stud. Surf. Sci. Catal.* **2000**, *129*, 837.

(33) Sakata, Y.; Uddin, M. A.; Muto, A.; Koizumi, K.; Kanada, Y.; Murata, K. *J. Anal. Appl. Pyrolysis* **1997**, *43*, 15.

(34) Satsuma, A.; Ebigase, T.; Inaki, Y.; Yoshida, H.; Kobayashi, S.; Uddin, M. A.; Sakata, Y.; Hattori, T. *Stud. Surf. Sci. Catal.* **2001**, *135*, 277.

(35) Yoshida, H.; Murata, C.; Inaki, Y.; Hattori, T. *Chem. Lett.* **1998**, 1121.

(36) Yoshida, H.; Kimura, K.; Inaki, Y.; Hattori, T. *Chem. Commun.* **1997**, 129.

(37) Inaki, Y.; Yoshida, H.; Hattori, T. *J. Phys. Chem. B* **2000**, *104*, 10304.

(38) Inaki, Y.; Yoshida, H.; Kimura, K.; Inagaki, S.; Fukushima, Y.; Hattori, T. *Phys. Chem. Chem. Phys.* **2000**, *2*, 5293.
(39) Ivin, K. J.; Mol, J. C. *Olefin metathesis and metathesis polymerization*; Academic Press: San Diego, 1997.
(40) Ivin, K. J.; Rooney, J. J.; Stewart, C. D. *J. Chem. Soc., Chem. Commun.* **1978**, 604.
(41) Ahn, H.-G.; Yamamoto, K.; Nakamura, R.; Niiyama, H. *Chem. Lett.* **1992**, 503.
(42) Buchacher, P.; Fischer, W.; Aichholzer, K. D.; Stelzer, F. *J. Mol. Catal.* **1996**, *115*, 163.
(43) Jannini, M. J. D. M.; Buffon, R.; de Wit, A. M.; Mol, J. C. *J. Mol. Catal. A* **1998**, *133*, 201.
(44) Buffon, R.; Jannini, M. J. D. M.; Abras, A.; Mol, J. C.; de Wit, A. M.; Kellendonk, F. J. A. *J. Mol. Catal. A* **1999**, *149*, 275.
(45) Chuang, I.-S.; Maciel, G. E. *J. Phys. Chem. B* **1997**, *101*, 3052.
(46) Morrow, B. A.; Cody, I. A.; Lee, L. S. M. *J. Phys. Chem.* **1975**, *79*, 2405.
(47) Morrow, B. A.; Cody, I. A. *J. Phys. Chem.* **1976**, *80*, 1995.
(48) Morrow, B. A.; Cody, I. A.; Lee, L. S. M. *J. Phys. Chem.* **1976**, *80*, 1998.
(49) Morrow, B. A.; Cody, I. A.; Lee, L. S. M. *J. Phys. Chem.* **1976**, *80*, 2761.
(50) Bunker, B. C.; Haaland, D. M.; Ward, K. J.; Michalske, T. A.; Smith, W. L. *Surf. Sci.* **1989**, *210*, 406.
(51) Michalske, T. A.; Bunker, B. C. *J. Appl. Phys.* **1984**, *56*, 2686.
(52) Bunker, B. C.; Haaland, D. M.; Michalske, T. A.; Smith, W. L. *Surf. Sci.* **1989**, *222*, 95.
(53) Morrow, B. A.; Devi, A. *J. Chem. Soc., Faraday Trans. 1* **1972**, *68*, 403.
(54) Yoshida, H.; Murata, C.; Hattori, T. *J. Catal.* **2000**, *194*, 364.
(55) Morrow, B. A. *Stud. Surf. Sci. Catal.* **1990**, *57*, A161.
(56) Silverstein, R. M.; Webster, F. X. *Spectrometric Identification of Organic Compounds*, 5th ed.; Wiley: New York, 1997.
(57) Peri, J. B. *J. Phys. Chem.* **1966**, *70*, 2937.
(58) Low, M. J. D.; Ramasubramanian, N.; Subba Rao, V. V. *J. Phys. Chem.* **1967**, *71*, 1726.
(59) Eischens, R. P.; Pliskin, W. A. *Adv. Catal.* **1958**, *10*, 1.
(60) Blomfield, G. A.; Little, L. H. *Can. J. Chem.* **1973**, *51*, 1771.
(61) The fitting by 3 or 5 Gaussian curves did not give a good result, and the fitting by 4 curves was enough to produce a line shape similar to the spectrum. These curve fitting results do not rule out the possibility that more than 4 bands exist; for example, some bands might overlap at the band of lowest energy (258 nm, 4.8 eV), since this band is broad in comparison with others.
(62) Skuja, L. *J. Non-Cryst. Solids* **1998**, *239*, 16, and references therein.
(63) Griscom, D. L. *J. Ceram. Soc. Jpn.* **1991**, *99*, 923.
(64) Tohmon, R.; Mizuno, H.; Ohki, Y.; Sasagane, K.; Nagasawa, K.; Hama, Y. *Phys. Rev. B* **1989**, *39*, 1337.
(65) Stapelbroek, M.; Griscom, D. L.; Friebele, E. J.; Sigel, G. H., Jr. *J. Non-Cryst. Solids* **1979**, *32*, 313.
(66) Dutt, D. A.; Higby, P. L.; Griscom, D. L. *J. Non-Cryst. Solids* **1991**, *130*, 41.
(67) Hosono, H.; Yamazaki, K.; Abe, Y. *J. Am. Ceram. Soc.* **1987**, *70*, 867.
(68) Schnadt, R.; Ruber, A. *Solid State Commun.* **1971**, *9*, 159.
(69) Skuja, L. *Solid State Commun.* **1992**, *84*, 613.
(70) Skuja, L. *J. Non-Cryst. Solids* **1994**, *179*, 51.
(71) Skuja, L. *Defect in SiO_2 and Related Dielectrics*: *Science and Technology*; Pacchioni, G. et al., Eds.; Kluwer Academic Publishers: Dordrecht, The Netherlands, 2000; p 73.
(72) Devine, R. A. B.; Arndt, J. *Phys. Rev. B* **1989**, *39*, 5132.
(73) Imai, H.; Hirashima, H. *J. Non-Cryst. Solids* **1994**, *179*, 202.
(74) Hibino, Y.; Hanafusa, H. *J. Appl. Phys.* **1986**, *60*, 1797.
(75) Glinka, Y. D.; Lin, S.-H.; Hwang, L.-P.; Chen, Y.-T. *J. Phys. Chem. B* **2000**, *104*, 8652.